

## STUDY OF SOME FACTORS AFFECTING DETERMINATION OF DYNAMIC ELASTIC CONSTANTS OF ROCKS

---

**ELSEMAN I. ABDEL-RASOUL,**

Associate Professor, Mining and Metallurgical Eng. Dept., Faculty of Engineering, Assiut University, [elseman1@yahoo.com](mailto:elseman1@yahoo.com).

(Received September 5, 2007 Accepted September 25, 2007)

*Measurements of the seismic wave velocities as well as the density of the rock material are necessary for calculating dynamic elastic constants. Correct determination of the dynamic elastic constants is the base for correct calculation of dynamic strains and stresses. These calculations use equations that have been formulated according to some assumptions. This study investigates the effect of the assumptions of 1-D and 3-D wave propagation on the magnitudes of the estimated dynamic elastic constants. Also some relations between densities, seismic velocities, velocity ratio, Poisson's ratio, Young's modulus, and shear modulus will be developed. The study depicted a significant effect of the assumption of 1-D or 3-D wave propagation on the calculated magnitudes of the dynamic elastic constants and came up with some useful relationships between the above mentioned parameters.*

**KEYWORDS:** Rock density, seismic wave velocities, dynamic elastic constants, dynamic stress and strain.

### INTRODUCTION

The knowledge of mechanical and elastic properties is essential in any rock mechanics investigations related to mining, tunneling, drilling, blasting, cutting, or crushing. For example, estimation of the level of the dynamic strains and stresses induced by ground vibrations due to blasting operations in mines and quarries is of concern to the mining, civil, and geological engineers. The reason is that these strains and stresses may cause damage to mining structures such as high walls and mine openings or nearby structures such as dwelling buildings, bridges, dams, tunnels, pipelines, and underground power stations. To estimate these dynamic strains and stresses, bulk density, dynamic elastic constants and/or seismic wave velocities should be available. Measurements of the ground peak particle velocities at the locations of interest should be available as well. The elastic properties of rock materials are either evaluated from the conventional geotechnical methods or the in-situ geophysical measurements. Shallow geophysical techniques are considered as one of the accurate and cost effective methods used in engineering site characterization of the rock mass. They are an alternative means of the conventional geotechnical ones, which are sometimes tedious and very expensive. The rock mass quality depends mainly upon the material elastic constants, which include shear modulus (G), Poisson's ratio ( $\nu$ ) and Young's modulus (E) [1-10].

Rock dynamic elastic constants are calculated from the longitudinal wave velocity ( $C_p$ ), shear wave velocity ( $C_s$ ) and density ( $\rho$ ). Generally, seismic wave velocities are higher for more dense and compact rocks than less dense and compact rocks; fine-grained than coarse-grained rocks; higher density than lower density rocks; lower porosity than higher porosity rocks; higher confining than lower confining pressures; lower temperature than higher temperature; and parallel to than perpendicular to bedding planes. The resonance and ultrasonic pulse methods are used to determine the elastic wave velocities in laboratory. The two methods do not give equivalent results even in nearly isotropic rocks. Although the discrepancy between the two methods probably is not of great significance in E and G determinations (about 6%), it may be significant regarding  $\nu$  determinations (could reach 24%). Consequently, while either method might provide an adequate estimation of E and G,  $\nu$  ratio determination by the resonance method is not recommended because of uncertainty with its determination. Seismic wave propagation method is used for field determinations of dynamic elastic constants. If the environmental conditions in the laboratory and in situ are the same, the results are comparable [11].

Usually E and G values obtained by dynamic methods are higher than those obtained by static techniques (both in the laboratory and in situ tests). The greater the degree of rock compactness, the more nearly dynamic and static elastic constants may agree. Static constants give rise to large scatter of results, but can be extended to the high strains  $10^{-2}$  occurring in mining processes. In dynamic methods, low strains of  $10^{-5}$  are involved with high rates of loading and scatter is comparatively small. Since dynamic methods usually involve low stresses, a comparison of static and dynamic values of E is meaningful only if the values of the static E are taken at comparable stress levels, i.e., using initial or zero stress tangent modulus. The static elastic modulus ranged from one-sixteenth to one-third of the seismic values [11].

In most cases, the values of the ratio of  $C_s / C_p$  vary within a narrow range in crystalline and metamorphic rocks, between 1.7 and 1.9. The range of variation of this ratio is wider for sedimentary rocks (from 1.5 to 1.4), owing to the low shear strength of weak and porous rocks ( $\nu$  approaches 0.5). The value of this velocity ratio is very high for argillaceous rocks, and tends to infinity in friable rocks. It should be noted that seismic velocities does not depend on frequency in practice, so that it is possible to employ any frequency of vibrations in research [12].

Dowding mentioned that using bar velocity in calculating E is accurate enough for engineering applications [1]. Also, Coates [5] concluded that using bar velocity in calculating E or vice versa, would produce an answer about 5% higher than using longitudinal wave velocity. Abdel-Rasoul and Omran [7] observed that E is higher in case of using bar velocity than in case of using longitudinal wave velocity. Also, they observed that the percentage of E-increase increases with increasing Poisson's ratio.

## AIM OF THE RESEARCH

Calculations of the dynamic strains and stresses are based on predetermined dynamic elastic constants ( $\nu$ , E and G). Determination of these dynamic elastic constants depends on assumptions, measurements (rock density and seismic wave velocities) and calculation procedures. This paper investigates the effect of the assumption of 1-

D or 3-D wave propagation on the magnitudes of the dynamic elastic constants. Also, interrelations between rock densities,  $C_p$ ,  $C_s$ ,  $C_s/C_p$ ,  $\nu$ ,  $E$ ,  $G$ , and  $\nu$ -factor as well as the calculation procedures would be investigated.

## RELATIONS BETWEEN $C_p$ , $C_s$ , DYNAMIC ELASTIC CONSTANTS, STRAINS AND STRESSES

In derivation of the following relations, it is assumed that the rock material is homogeneous, isotropic, and perfectly elastic.

### Relations between $C_p$ , $C_s$ and Dynamic Elastic Constants [1, 5, 7-12]:

Bar velocities (1-D) are given by:

$$C_p = (E / \rho)^{1/2} \quad (1)$$

From which, Young's Modulus is:

$$E = \rho C_p^2 \quad (2)$$

The longitudinal wave propagation velocities (3-D) are related to the elastic constants by the following equation:

$$(C_p)^2 = (1 - \nu) E / [(1 + \nu) (1 - 2 \nu) \rho] \quad (3)$$

From which,  $E$  is:

$$E = \rho (C_p)^2 [(1 + \nu) (1 - 2 \nu) / (1 - \nu)] \quad (4)$$

Shear wave velocity is given by the equation:

$$C_s = (G / \rho)^{1/2} \quad (5)$$

From which, shear modulus (3-D) is:

$$G = \rho C_s^2 \quad (6)$$

Also, we have the following expression for shear wave velocity:

$$(C_s)^2 = E / [2 (1 + \nu) \rho] \quad (7)$$

With some manipulation between equation (3) and equation (7), we can find the following equation for calculating  $\nu$ :

$$\nu = [1 - 2 (C_s / C_p)^2] / [2 - 2 (C_s / C_p)^2] \quad (8)$$

And

$$C_s = [(1 - \nu) / (1/2 - \nu)]^{1/2} \quad (9)$$

In case of  $\nu = 0.25$ , the  $C_p / C_s$  ratio is equal to 1.7. Also  $E$  and  $G$  are related by the following equation:

$$G = E / 2(1 + \nu) \quad (10)$$

### Dynamic Strains and Stresses [1, 5]:

Young's modulus (in uniaxial compression or tensile tests) is defined as:

$$E = \sigma / \epsilon \quad (11)$$

i.e.  $\sigma = E \epsilon \quad (12)$

And the normal (longitudinal) strain is defined as:

$$\varepsilon = \dot{u}_p / C_p \quad (13)$$

Using equations (2), (12), and (13), normal stress,  $\sigma$  can be expressed as:

$$\sigma = \rho C_p \dot{u}_p \quad (14)$$

Also, shear modulus,  $G$ , is defined as:

$$G = \tau / \gamma \quad (15)$$

$$\text{i.e. } \tau = G \gamma \quad (16)$$

And shear strain is defined as:

$$\gamma = \dot{u}_s / C_s \quad (17)$$

Using equations (6), (16), and (17), shear stress,  $\tau$  can be expressed as:

$$\tau = \rho C_s \dot{u}_s \quad (18)$$

Where:

$\varepsilon$  = normal strain

$\sigma$  = normal stress

$\dot{u}_p$  = longitudinal particle velocity.

$\dot{u}_s$  = transverse (shear) particle velocity

$\gamma$  = shear strain

$\tau$  = shear stress

## CALCULATION OF $C_S/C_P$ , $\nu$ , $\nu$ -FACTOR, E AND G

We have collected rock density,  $C_p$  and  $C_s$  for rocks from different sources. Some data contain field measurements of  $C_p$  and  $C_s$  [4, 6, 7, 14] while other data contain laboratory measurements of  $C_p$  and  $C_s$  [11]. Another group of data is provided as an average and it could be a mix of field and laboratory measurements [13]. We have calculated  $C_s/C_p$  and  $\nu$  (using equation (8)) for these data. Summary of these calculations is provided in **Table 1**. The last term in equation (4) has been called Poisson's Ratio Factor and is defined as:

$$\nu\text{-factor, } F = [(1 + \nu) (1 - 2 \nu) / (1 - \nu)] \quad (19)$$

Its magnitude has been calculated for all rocks and it is provided in **Table 2**.

E has been calculated using two methods. In the first method, E has been calculated using bar velocity, equation (2) based on the assumption of 1-D wave propagation ( $E_{1-D}$ ). In the second method, E has been calculated using longitudinal wave velocity as defined in equation (4) and based on the assumption of 3-D wave propagation ( $E_{3-D}$ ). It is observed that  $E_{1-D}$  is greater than  $E_{3-D}$ . The percentage of increase has been calculated as:

$$E\text{-Increase\%} = [E_{1-D} - E_{3-D}] \times 100 / E_{3-D} \quad (20)$$

Calculations of E are summarized in **Table 2**.

G has been calculated using three methods. In the first method, we used  $E_{1-D}$  in equation (10) to calculate G (being based on 1-D wave propagation, we called it  $G_{1-D}$ ). In the second method, we used  $E_{3-D}$  in equation (10) to calculate G. Being calculated on the 3-D wave propagation assumption; we called it  $G_{3-D}$ . In the third method, we

used  $C_s$  in equation (6) to calculate  $G$  (called  $G_{3-D(cs)}$  or  $G_{cs}$ ). Results of  $G$  calculations are provided in **Table 2**. In the table, it can be seen that the second and third methods produce the same  $G$  magnitudes. That is because the two methods are based on the 3-D wave propagation assumption. Also, it can be seen that  $G_{1-D}$  is greater than  $G_{3-D}$ . That is because we used  $E_{1-D}$  in equation (10) which is based on the assumption of 1-D wave propagation. The percentage of  $G$  increase is calculated as:

$$G\text{-Increase}\% = [G_{1-D} - G_{3-D}] \times 100 / G_{3-D} \quad (21)$$

Results of these calculations are provided in **Table 2**.

**Table 1:** Summary of rock density,  $C_p$ ,  $C_s$ , and calculations of  $C_s/C_p$  and  $\nu$ .

Serial No.	Rock Type	Density, kg/m <sup>3</sup>	$C_p$ , m/sec	$C_s$ , m/sec	$C_s/C_p$	Poisson's Ratio, $\nu$
<b>Abdel-Rasoul and Omran [7]</b>						
1	Limestone, layer 1	2000	1661	1038	0.6249	0.180
2	Limestone, layer 1	2000	1612	1003	0.6222	0.178
3	Limestone, layer 2	2200	2838	1715	0.6043	0.212
4	Limestone, layer 2	2200	2480	1649	0.6649	0.104
5	Limestone, layer 3	2200	4604	3081	0.6692	0.094
6	Limestone, layer 3	2200	4380	2933	0.6696	0.0935
<b>Tealeb et al [6]</b>						
7	Weathered Limestone	2400	385	226	0.5870	0.237
8	Foundation Limestone	2400	952	560	0.5882	0.235
<b>Burgher [4]</b>						
9	Montana mine rocks	2610	2487	1463	0.5883	0.235
<b>Kabongo [14]</b>						
10	Coal	1475	3800	2400	0.6316	0.168
<b>Atlas Powder [13]</b>						
11	Granite	2670	5029	2743	0.5454	0.288
12	Gabbro	2980	6553	3444	0.5256	0.309
13	Basalt	3000	5608	3048	0.5435	0.290
14	Dunite	3280	7985	4084	0.5115	0.323
15	Sandstone	2450	3353	1981	0.5908	0.232
16	Limestone	2650	4572	2972	0.6500	0.134
17	Shale	2350	2895	1676	0.5790	0.248
18	Slate	2800	3962	2865	0.7231	0.047
19	Marble	2750	5791	3505	0.6052	0.211
20	Schist	2800	4541	2895	0.6375	0.158

Table 1: ...continued

Serial No.	Rock Type	Density, kg/m <sup>3</sup>	C <sub>p</sub> , m/sec	C <sub>s</sub> , m/sec	C <sub>s</sub> /C <sub>p</sub>	Poisson's Ratio, $\nu$
<b>Lama and Vutukuri [11]</b>						
21	Hornblende Schist	2990	6090	3720	0.6108	0.202
22	Granulite	3053	6310	3390	0.5372	0.297
23	Hornblende Schist	3052	6340	3980	0.6378	0.186
24	Hornblende Schist	2737	6300	3920	0.6222	0.184
25	Hornblende Schist	3011	6690	3670	0.5486	0.285
26	Hornblende Schist	2961	6730	4000	0.5944	0.227
27	Dolerite	3106	5220	3340	0.6398	0.153
28	Uralite diabase	3162	6130	3130	0.5106	0.324
29	Hornblendite	3247	5630	3630	0.6448	0.144
30	Dolerite	3000	6370	3440	0.5400	0.294
31	Hornblende granulite	3042	6700	3590	0.5358	0.299
32	Hornblende schist	3198	5840	3530	0.6045	0.212
33	Hornblende schist	3031	6360	3750	0.5896	0.225
34	Hornblendite	3472	6390	3290	0.5149	0.320
35	Dolerite	3136	6480	3730	0.5756	0.252
36	Vein quartz	2796	5210	2840	0.5451	0.289
37	Hornblende granulite	3084	6110	3710	0.6072	0.208
38	Hornblende schist	3011	5750	3700	0.6435	0.154
39	Uralite basalt	3062	6580	3660	0.5562	0.276
40	Uralite basalt	2672	5010	3160	0.6307	0.170
41	Dolerite	3111	5590	3300	0.5903	0.233
42	Granulite	3106	6150	3380	0.5496	0.284
43	Granulite	3356	5420	3150	0.5812	0.245
44	Uralite diabase	3000	6650	3710	0.5579	0.274
45	Dolerite	3011	5440	3500	0.6434	0.147
46	Uralite diabase	3057	6100	3840	0.6295	0.172
47	Tremolite schist	3011	6320	3460	0.5475	0.286

## ANALYSES AND DISCUSSIONS OF RESULTS

**Fig. 1** illustrates the relation between  $C_p$ ,  $C_s$ , and density. The relations have very good correlation coefficients ( $R=0.78$  for  $C_p$  and  $R=0.73$  for  $C_s$ ). These high correlation coefficients give us confidence in our data base and recommend the use of the relations to predict appreciable values for  $C_p$  and  $C_s$ . The relations show the increase of  $C_p$  and  $C_s$  with increasing density. At densities greater than about 2000 kg/m<sup>3</sup>, the rate of increase of  $C_s$  decreases compared to the rate of increase of  $C_p$ .

**Table 2:** Summary of the calculations of  $\nu$ -factor; dynamic E and G by different methods.

Serial No.	$\nu$ -Factor, F	Young's Modulus, E, $10^4$ kg/cm <sup>2</sup>			Rigidity Modulus, G, $10^4$ kg/cm <sup>2</sup>			
		E <sub>1-D</sub> , using equation (2)	E <sub>3-D</sub> , using equation (4)	E-increase, %	G <sub>1-D</sub> using E <sub>1-D</sub> & eq. (10)	G <sub>3-D</sub> using E <sub>3-D</sub> & eq. (10)	G <sub>Cs</sub> using C <sub>s</sub> & eq. (6)	G-increase, %
<b>Abdel-Rasoul and Omran [7]</b>								
1	0.921	5.625	5.180	8.58	2.383	2.195	2.197	8.5
2	0.9229	5.298	4.889	8.35	2.249	2.075	2.076	8.3
3	0.8859	18.063	16.002	12.9	7.452	6.602	6.596	13.0
4	0.9759	13.793	13.46	2.47	6.247	6.096	6.098	6.1
5	0.9805	47.536	46.613	1.98	21.726	21.304	21.288	2.1
6	0.9807	43.023	42.193	1.97	19.672	19.293	19.292	2.0
<b>Tealeb et al [6]</b>								
7	0.8528	0.363	0.309	17.3	0.1466	0.125	0.125	17.3
8	0.8556	2.217	1.897	16.9	0.8977	0.768	0.767	17.0
<b>Burgher [4]</b>								
9	0.8556	16.451	14.076	16.9	6.6602	5.699	5.696	16.9
<b>Kabongo [14]</b>								
10	0.9322	21.712	20.239	7.28	9.2943	8.664	8.661	7.32
<b>Atlas Powder [13]</b>								
11	0.7670	68.834	52.796	30.4	26.721	20.495	20.478	30.5
12	0.7236	130.445	94.396	38.2	49.826	36.056	36.031	38.3
13	0.7631	96.176	73.392	31.0	37.278	28.447	28.411	31.2
14	0.6918	213.184	147.48	44.6	80.568	55.736	55.767	44.5
15	0.8598	28.078	24.142	16.3	11.395	9.798	9.801	16.3
16	0.9585	56.466	54.125	4.3	24.897	23.865	23.860	4.4
17	0.8364	20.077	16.793	19.6	8.044	6.728	6.729	19.5
18	0.9954	44.804	44.598	0.00	21.396	21.298	23.428	0.0
19	0.8871	94.009	83.400	12.7	34.438	34.434	34.438	12.7
20	0.9407	58.856	55.366	6.3	23.921	23.906	23.921	6.2

**Fig. 2** and **Fig. 3** present the relations between E<sub>1-D</sub>, E<sub>3-D</sub>; G<sub>1-D</sub>, G<sub>3-D</sub>, and Poisson's ratio. Despite the low correlation coefficients (R=0.54, 0.34, 0.46, and 0.26 respectively), the figures do show the increase of E and G with increasing Poisson's

ratio. Also, the figures show that the difference between 1-D and 3-D magnitudes increases with increasing Poisson's ratio.

**Table 2:** ...continued.

Serial No.	ν-Factor, F	Young's Modulus, E, 10 <sup>4</sup> kg/cm <sup>2</sup>			Rigidity Modulus, G, 10 <sup>4</sup> kg/cm <sup>2</sup>			
		E <sub>1-D</sub> , using eq. (2)	E <sub>3-D</sub> , using eq. (4)	E-increase, %	G <sub>1-D</sub> using E <sub>1-D</sub> & eq. (10)	G <sub>3-D</sub> using E <sub>3-D</sub> & eq. (10)	G <sub>C<sub>s</sub></sub> using C <sub>s</sub> & eq. (6)	G-increase, %
<b>Lama and Vutukuri [11]</b>								
21	0.8977	113.041	101.481	11.4	47.022	42.213	42.178	11.5
22	0.7490	123.913	92.811	33.5	47.769	35.779	35.765	33.6
23	0.9150	125.053	114.423	9.3	52.810	48.321	49.281	7.2
24	0.9170	110.736	101.547	9.1	46.763	42.883	42.872	9.1
25	0.7728	137.371	106.160	29.4	53.452	41.307	41.340	29.3
26	0.8667	136.710	118.483	15.4	55.709	48.282	48.294	15.4
27	0.9447	86.273	81.504	5.9	37.412	35.344	35.320	5.9
28	0.6894	121.120	83.502	45.1	45.740	31.534	31.578	44.9
29	0.9516	104.913	99.830	5.1	45.854	43.632	43.614	5.1
30	0.7551	124.088	93.704	32.4	47.948	36.207	36.188	32.5
31	0.7449	139.200	103.695	34.2	53.578	39.913	39.965	34.1
32	0.8859	111.182	98.500	12.9	45.867	40.635	40.622	12.9
33	0.8694	124.977	108.650	15.0	51.011	44.347	43.449	17.4
34	0.6988	144.515	100.990	43.1	54.740	38.254	38.309	42.9
35	0.8302	134.232	111.440	20.5	53.607	44.505	44.476	20.5
36	0.7651	77.365	59.189	30.7	30.010	22.959	22.988	30.5
37	0.8907	117.362	104.540	12.3	48.577	43.270	43.271	12.3
38	0.9439	101.479	95.7897	5.9	43.969	41.503	42.019	4.6
39	0.7859	135.141	106.202	27.3	52.955	41.615	41.812	26.7
40	0.9304	68.366	63.606	7.5	29.216	27.182	27.198	7.4
41	0.8584	99.096	85.068	16.5	40.185	34.496	34.535	16.4
42	0.7747	119.752	92.772	29.1	46.632	36.126	36.171	28.9
43	0.841	100.497	84.517	18.9	40.360	33.943	33.945	18.9
44	0.7932	135.237	107.267	26.1	53.076	42.099	42.092	26.1
45	0.9493	90.832	86.230	5.3	39.596	37.589	37.599	5.3
46	0.9285	115.954	107.668	7.7	49.469	45.934	45.950	7.7
47	0.8645	122.596	105.984	15.7	47.666	41.207	36.745	29.7

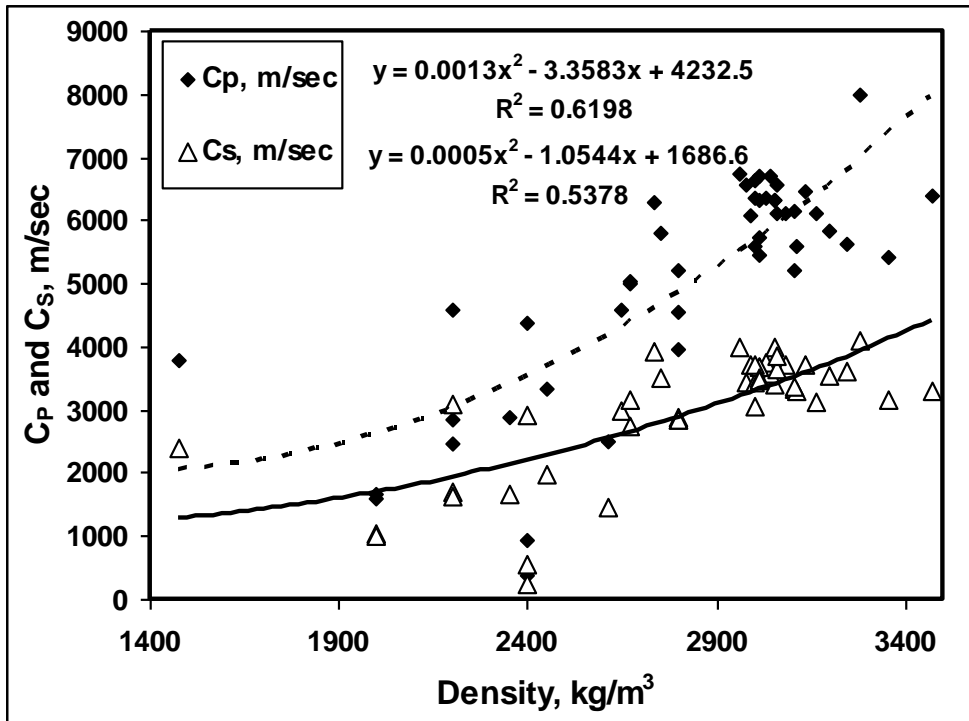


Fig. 1: Relations between  $C_P$  (dashed line),  $C_S$  (solid line), and density.

To clarify the differences between E and G magnitudes based on the assumptions of 1-D and 3-D wave propagation, we have plotted E-Increase% and G-Increase% versus  $C_S/C_P$ ,  $\nu$  and  $\nu$ -factor in Fig.4. The figure provides us with very useful information. Firstly, the correlation factors for the six relations are almost equal to one. Secondly, the increase% for E and G is almost the same (data points coincide). Thirdly, the increase in E and G magnitudes due to the assumption of 1-D wave propagation can go up to more than 45%. In fact, most of the rock population lies in this range. This is a warning that we should not rely on the old saying that the difference between 1-D and 3-D calculations is not significant and it may be within 5% [1, 5]. The figure shows that the difference bypasses 5% if  $C_S/C_P$  is less than 0.65, or  $\nu$  is greater than 0.15, or  $\nu$ -factor is less than 0.96. The difference increases with increasing  $\nu$  and decreases with increasing  $C_S/C_P$  ratio and  $\nu$ -factor. The figure can be used to check if the difference between 1-D and 3-D calculations exceeds 5% or not. Indeed, the calculations based on 3-D assumption are better when it comes to field applications. Also, the higher calculated elastic constants will produce higher stress magnitudes. As the 3-D calculations are better for field applications, we have plotted  $E_{3-D}$  and  $G_{3-D}$  versus density,  $C_P$  and  $C_S$  in Fig. 5. Density,  $C_P$  and  $C_S$  are measured quantities and constitute the input on which the whole E, G, strain, and stress calculations are based. If the engineering project is at the early stage of feasibility study and measurement facilities are not available or the monetary funds are not enough at that stage, Fig. 5 can be used to estimate E and G even by just knowing the density. Fortunately, the correlation coefficients are excellent ranging from 0.83 to 0.99.

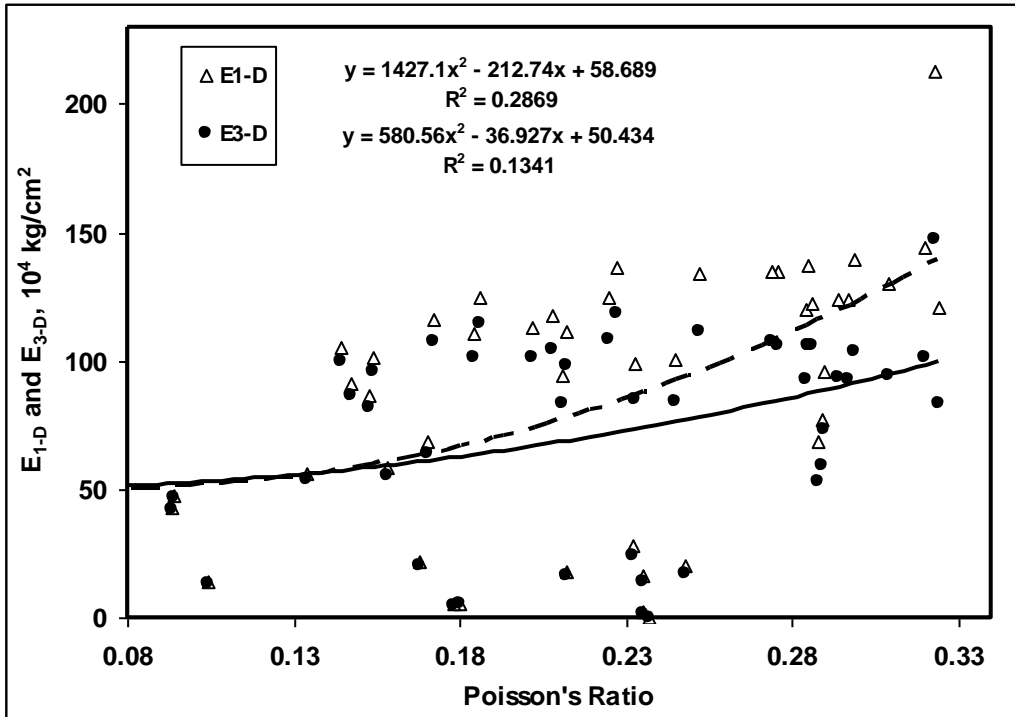


Fig. 2: Relations between  $E_{1-D}$  (dashed line),  $E_{3-D}$  (solid line), and  $\nu$ .

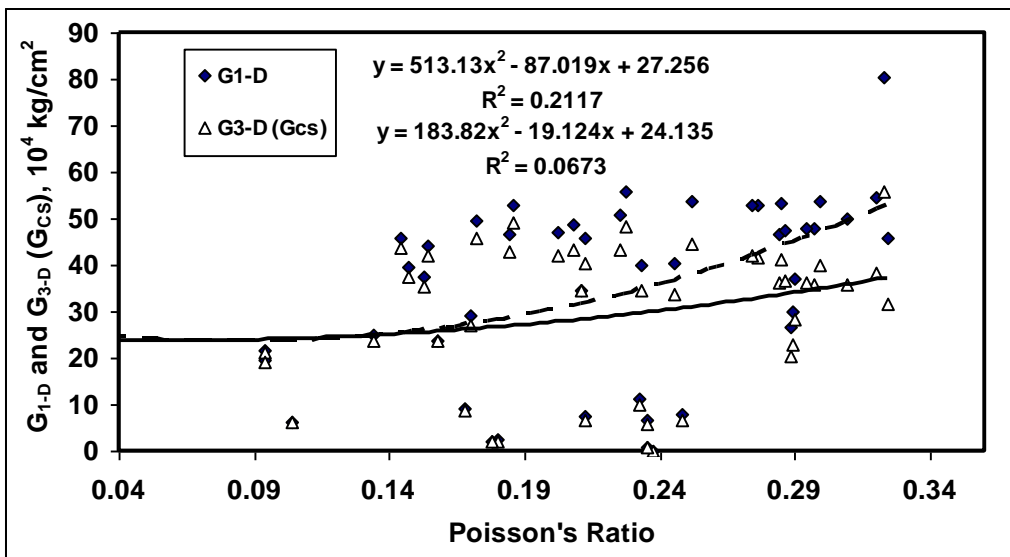


Fig. 3: Relations between  $G_{1-D}$  (dashed line),  $G_{3-D}$  (solid line), and  $\nu$ .

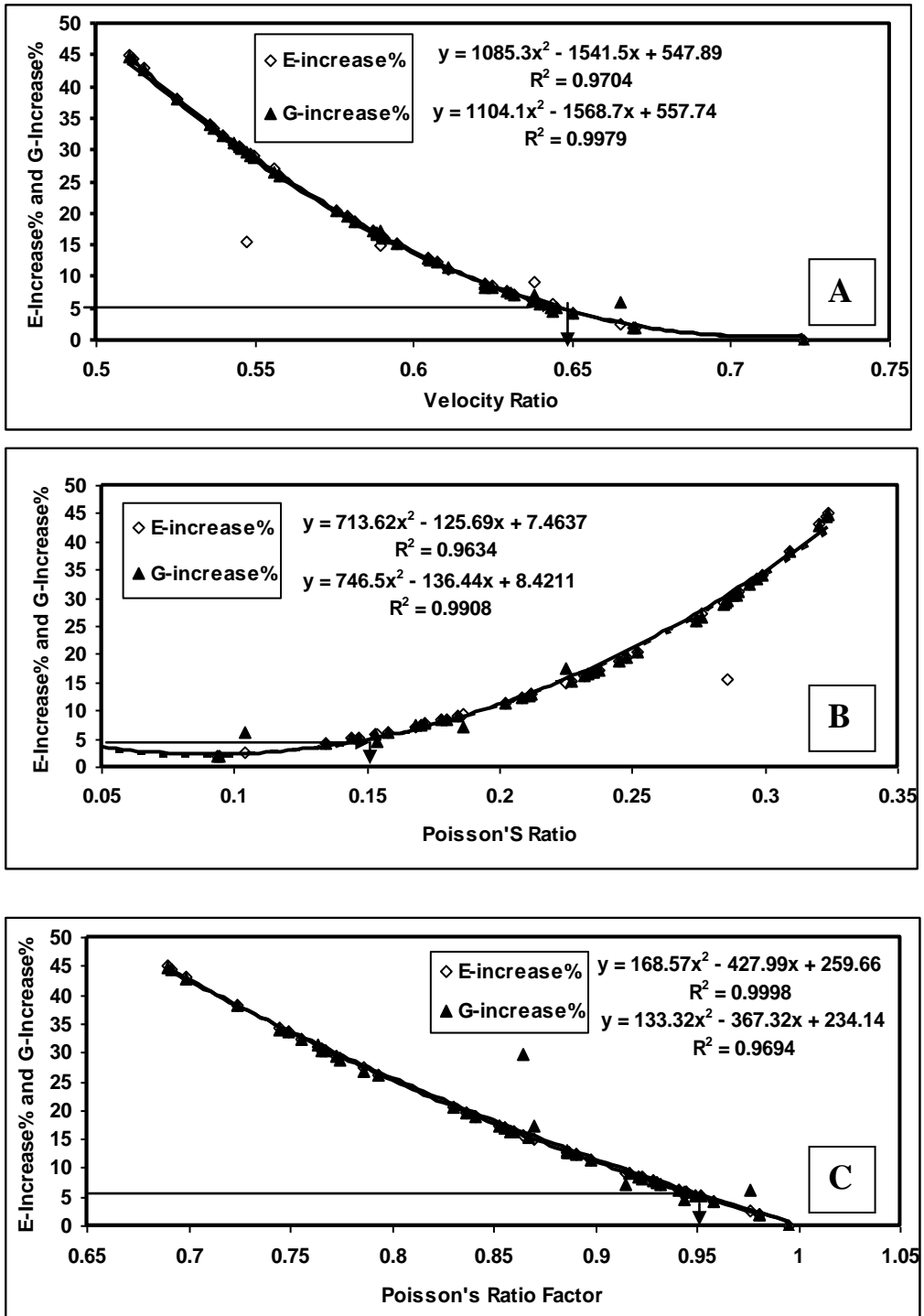


Fig. 4: Relations between E-Increase & G-Increase,  $C_s/C_p$  ratio (A),  $\nu$  (B), and  $\nu$ -factor (C).

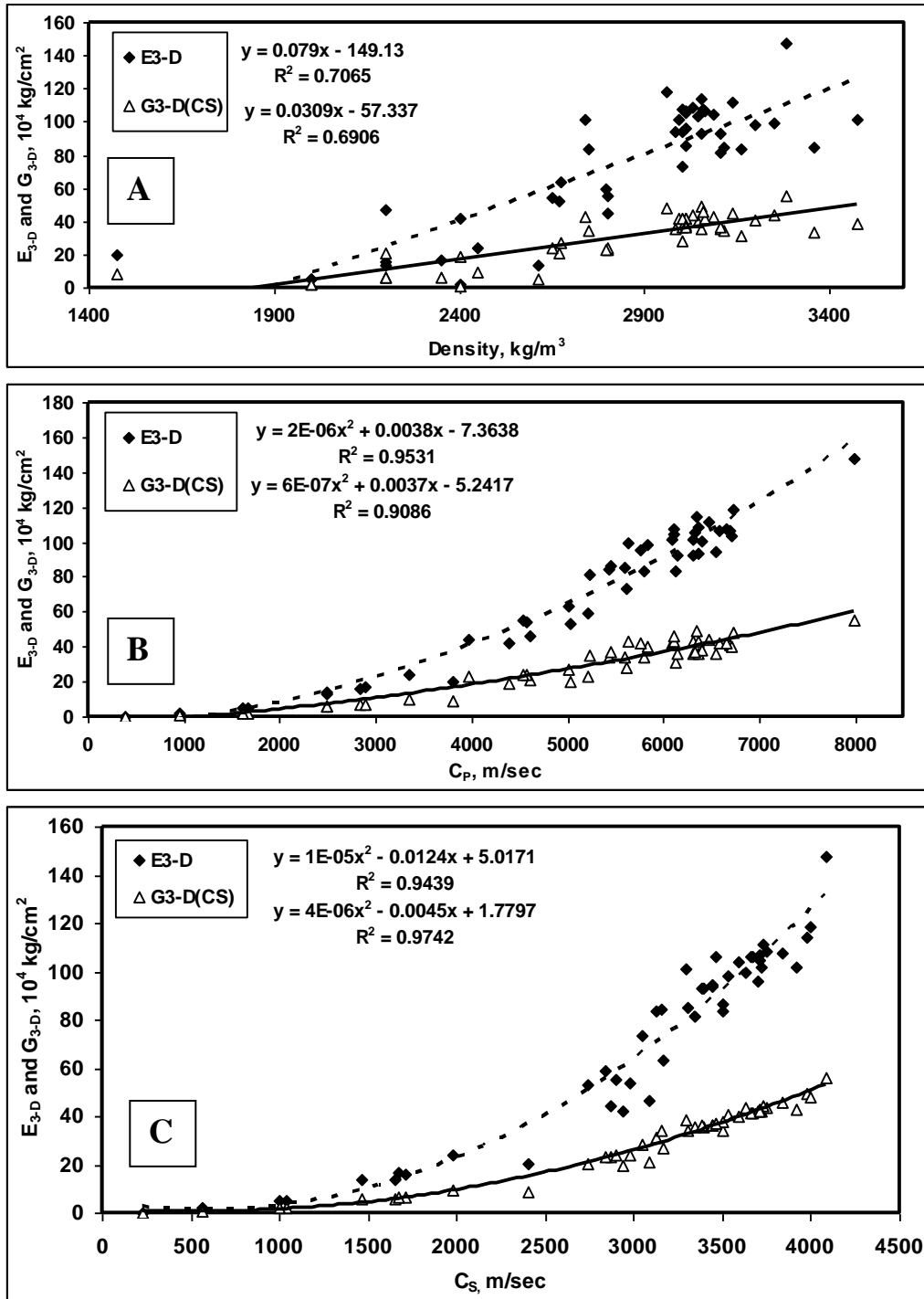


Fig. 5: Relations between  $E_{3-D}$  (dashed line) &  $G_{3-D}$  (solid line); density (A),  $C_p$  (B) and  $C_s$  (C).

Having illustrated the impact of the assumption of 1-D and 3-D wave propagation on the magnitudes of E and G, it is time to look at stress calculations. Equation (18), as it is, is providing shear stresses based on 3-D wave propagation. However, using equation (10) for G-calculations will produce either  $G_{1-D}$  (by plugging  $E_{1-D}$ ) or  $G_{3-D}$  (by plugging  $E_{3-D}$ ). Hence, one should be aware of that. Considering normal stresses calculated from equation (14), it is based on the assumption of 1-D wave propagation. That is because it is derived from in equation (1), an expression for bar velocity. Accordingly, normal stresses have to be corrected using **Fig. 4** if 3-D magnitudes are required. A more appropriate solution to have peace of mind is attained by modifying equation (14) to directly estimate normal stresses using 3-D wave propagation assumption. This can be done by multiplying equation (14) by the  $\nu$ -factor to be in the form:

$$\sigma = \rho C_p \dot{u}_p \times [(1 + \nu) (1 - 2 \nu) / (1 - \nu)] \quad (22)$$

In other words, we used equation (4) and equation (13) to derive equation (22).

## CONCLUSIONS AND RECOMMENDATIONS

The paper has illustrated the effect of procedure of calculation and the assumptions of 1-D and 3-D wave propagation on the calculated magnitudes of dynamic E, G and stresses. Also, statistical interrelations between rock density, seismic velocity, velocity ratio, Poisson's ratio, and dynamic elastic constants have been derived. From the results of the performed comparisons, calculations, and analyses some conclusions and recommendations have been drawn:

- 1- Magnitudes of dynamic E and G are higher when calculated using 1-D wave propagation assumption than when they are calculated on the 3-D wave propagation basis.
- 2- The difference between 1-D and 3-D calculations is the same for both E and G.
- 3- The difference increases with increasing Poisson's ratio, with decreasing  $C_s/C_p$  ratio and decreasing  $\nu$ -factor of the rock material.
- 4- The difference exceeds 5% for Poisson's ratio of magnitudes higher than 0.15, for  $C_s/C_p$  ratio less than 0.65, and for  $\nu$ -factor less than 0.96. The difference can be more than 45%.
- 5- Dowding's expression for calculating normal stresses has been modified to get 3-D magnitudes by multiplying it by the  $\nu$ -factor.
- 6- Good statistical relations have been obtained between factors affecting estimation of dynamic E and G and could be used for their estimation. These include:
  - i- Relations between  $C_p$  and density;  $C_s$  and density ( $R=0.78$  and  $0.73$  respectively).
  - ii- Relations between E-increase% and G-increase% versus  $C_s/C_p$  ratio,  $\nu$ -ratio, and  $\nu$ -factor ( $R$  for the six relations is almost one).
  - iii- Relations between  $E_{3-D}$  and  $G_{3-D}$  versus density,  $C_p$  and  $C_s$  ( $R$  ranges from 0.83 to 0.99).
- 7- High determined  $E_{1-D}$  and  $G_{1-D}$  magnitudes will cause higher estimated stresses than those estimated from  $E_{3-D}$  and  $G_{3-D}$ . When considering the safe limit of

blasting vibrations damage criteria, stresses estimated using  $E_{1-D}$  and  $G_{1-D}$  will be more conservative.

## REFERENCES

1. Dowding, Charles, "Ground vibration monitoring and control", Prentice Hall, USA, 297 p., (1985).
2. Siskind, D. E., Stagg, M. S., Kopp, J. W., and Dowding, C. H., "Structure response and damage produced by ground vibration from surface Mine blasting", RI 8507, USBM, 74 p., (1980).
3. Abdel-Rasoul, E. I., "Measurement and analysis of the effect of ground vibrations induced by blasting at the limestone quarries of the Egyptian Cement Company", Int. Conf. for Environmental Hazard Mitigation, Center of Environmental Hazard Mitigation, Cairo University, Cairo, Egypt, 15 p., (2000).
4. Burgher, K. E., "P-wave and S-wave velocity measurement for stress-strain analysis", 15th Conf. on Expl. and Blasting Tech., SEE, Ohio, USA, pp. 87-96, (1979).
5. Coates, D. F., "Rock mechanics principles", Monograph 874, CANMET Energy, Mines, and Resources Canada, Ottawa, Canada, Ch. 8, (1981).
6. Tealeb, A. A.; Sobaih, M. E.; Mohamed, A. A., and Abdel-Rahman, K., "Stress level estimation for the ground beneath the 15th of May City buildings, Helwan, Cairo, Egypt", Int. Conf. for Environmental Hazard Mitigation, Center of Environmental Hazard Mitigation, Cairo University, Cairo, Egypt, 29 p., September 9-12, (2000).
7. Elseman I. Abdel-Rasoul and Awad A. Omran, "Estimation of stress and strain levels induced by blasting vibrations using measured particle and propagation velocities at Bani Khalid quarry", J. of Eng. Sciences, Assiut University, Vol. 35, No. 4, pp. 1009-1021, (2007).
8. Reynolds, J. M., "An introduction to applied and environmental geophysics", John Wiley & Sons, Chichester, England, 796p., (1997).
9. Sheriff, R. E. and Geldart, L. P., "Exploration seismology, Vol. 1: History, theory and data acquisition", Cambridge University Press, Cambridge, 253 p., (1982).
10. Dobrin, M. B., "Introduction to geophysical prospecting", 3rd Ed., McGraw-Hill International Book Co., 630 p., (1976).
11. Lama, R. D. and Vutukuri, V. S., "Handbook on mechanical properties of rocks- Testing techniques and results", Vol. II, TRANS TECH PUBLICATIONS, Clausthal, Germany, 481 p., (1978).
12. Rzhevsky, V. and Novik, G., "The physics of rocks", MIR PUBLISHERS, Moscow, 319 p., (1971).
13. Atlas Powder Company, "Explosives and rock blasting", Field Tech. Operations", Atlas Powder Co., Dallas, Texas, USA, pp.321-411, (1987).
14. Kabongo, K. K., "Blasting induced damage in coal", Proc. of the 21st Conf. on Exp. and Blasting Tech., ISEE, Ohio, pp. 203-213, (1995).

## "دراسة بعض العوامل المؤثرة على تعيين ثوابت المرونة الديناميكية للصخور"

معرفة الخواص الميكانيكية وخواص المرونة للصخور تعتبر أساسية في أي بحث ميكانيكا صخور متصل بالمناجم، الأنفاق، الحفر، التفجير، القطع، أو الطحن. وتقدير مستوى الاجهادات والانفعالات الديناميكية الناتجة عن الاهتزازات الأرضية بسبب عمليات التفجير في المناجم يعتبر مثال على ذلك. تم عمل هذه الدراسة لالقاء الضوء على طريقة حساب الثوابت الديناميكية للمرونة والتي على أساسها يتم حساب هذه الاجهادات والانفعالات. وحيث أن حساب قيم الثوابت الديناميكية للمرونة يعتمد على قياس كثافة الصخر وسرعات الموجات السيزمية والبناء على بعض الفروض وأيضاً طريقة الحساب التي سيتم اتباعها، فإن هذه الدراسة تبحث تأثير فرض انتشار الموجة الأحادي والثلاثي الأبعاد على القيم المحسوبة لثوابت المرونة وكذلك تبحث الدراسة عن وجود علاقات بينية بين كثافة الصخر والسرعات السيزمية ونسبة سرعات موجات القص الى سرعات الموجات الطولية ونسبة بواسون ومعامل ينج ومعامل القص ومعامل نسبة بواسون وأيضاً طريقة الحساب.

كشفت الدراسة عن تأثير واضح لفرض انتشار الموجة الأحادي البعد على زيادة قيم الثوابت الديناميكية للمرونة مقارنة بقيمها في حالة فرض انتشار الموجة ثلاثي الأبعاد وبالتالي علي قيم الاجهادات الديناميكية المحسوبة منها. أيضاً تم ايجاد علاقات احصائية جيدة ذات معامل ارتباط احصائي قوي بين العوامل المؤثرة على ثوابت المرونة الميكانيكية وبالتالي يمكن استخدامها في استنباط العوامل المؤثرة أو ثوابت المرونة نظراً لقوة معاملات الارتباط الاحصائي لهذه العلاقات.